Acta Crystallographica Section D
Biological Crystallography
ISSN 0907-4449

The hydration structure of a Z-DNA hexameric duplex determined by a neutron diffraction technique

Toshiyuki Chatake,[a] Ichiro Tanaka,[b] Hisao Umino,[c,d] Shigeki Arai[d] and Nobuo Niimura[b,d]*

[a]Faculty of Pharmaceutical Sciences, Chiba Institute of Science, Choshi, Chiba 288-0025, Japan, [b]Institute of Applied Beam Science, Graduate School of Science and Engineering, Ibaraki University, Hitachi, Ibaraki 316-8511, Japan, [c]Advanced Technology Corporation, Tokai, Ibaraki 319-1111, Japan, and [d]Neutron Research Center, Japan Atomic Energy Research Institute, Tokai, Ibaraki 319-1195, Japan

Correspondence e-mail: niimura@mx.ibaraki.ac.jp

Received 17 April 2005
Accepted 17 May 2005

PDB References:
d(CGCGCG), neutron structure, 1v9g, r1v9gsf; X-ray structure, 1woe, r1woesf.

In order to reveal the hydration structure of Z-DNA, a neutron diffraction study has been carried out at 1.8 Å resolution on a Z-DNA hexamer d(CGCGCG). Neutron diffraction data were collected with the BIX-3 single-crystal diffractometer at the JRR-3 reactor in the Japan Atomic Energy Research Institute (JAERI) using a large crystal (1.6 mm^3) obtained from D_2O solution. It has been found that almost all the guanine bases have participated in H/D exchange at the C8—H8 group, consistent with the acidic nature of this bond. 44 water molecules were found in the nuclear density maps, of which 29 showed the entire contour of all three atoms (D—O—D). The remaining 15 water molecules had a simple spherical shape, indicating that they were rotationally disordered. An interesting relationship was found between the orientational disorder of the water molecules and their locations. Almost all water molecules in the minor groove were well ordered in the crystal, while 40% of the water molecules in the major groove were rotationally disordered. The hydrogen-bonding networks in the hydration shells have two structural aspects: flexibility and regularity.

1. Introduction

DNA is a flexible and dynamic molecule that takes on various helical conformations depending on different conditions (Leslie *et al.*, 1980; Dickerson *et al.*, 1982). In particular, the structure of the DNA hexamer d(CGCGCG), which was originally solved by Rich and coworkers, has an unusual conformation (Wang *et al.*, 1979). It has a zigzag arrangement of the backbone atoms in a left-handed helical arrangement and this conformation is now called Z-DNA. In the last two decades, biologists have found an association between Z-DNA and transcription (Schroth *et al.*, 1992; Liu & Wang, 1987; Lipps *et al.*, 1983) and have discovered Z-DNA-specific binding proteins such as ADAR1 (Schwartz *et al.*, 1999), ZALM1 (Schwartz *et al.*, 2001) and DsrD (Mizuno *et al.*, 2003). Therefore, Z-DNA is now believed to play an important biological role (Rich & Zhang, 2003).

Z-DNA is a stable form of an alternating dC-dG or dG-dC polynucleotide sequence induced by high salt concentrations (Thamann *et al.*, 1981) or by alcohol (Feigon *et al.*, 1984). When the 5′-position of the cytosine base is methylated, the Z-conformation is remarkably stable (Fujii *et al.*, 1982; Behe & Felsenfeld, 1981). This raises the interesting question of how such a transitional state of DNA can be stabilized. Previous X-ray crystallographic analyses of DNA oligomers demonstrated definite differences between the hydration structures of B-DNA (Drew & Dickerson, 1981) and Z-DNA (Wang *et al.*, 1979), suggesting a close relationship between the stability of each DNA conformation and its hydration pattern. Water

molecules mediate the formation of the DNA duplex *via* hydrogen bonds. In order to characterize such interactions, it is essential to know the orientations of the H atoms in these water molecules. The Z-DNA hexamer d(CGCGCG) has been investigated by extremely high-resolution X-ray crystallographic analyses (Tereshko *et al.*, 2001; Egli *et al.*, 1991; Gessner *et al.*, 1989). However, the directional information of the water molecules surrounding the Z-DNA is not well known, because the X-ray atomic form factor of a H atom is much smaller than those of other atoms. In contrast, the neutron scattering lengths for H and D atoms are comparable to those of non-H atoms. Indeed, details of protein hydration can be observed even at medium resolution using the neutron diffraction technique (Chatake, Ostermann *et al.*, 2003). Previous neutron studies of polynucleotides have been limited to a fibre-diffraction study. Fourier difference syntheses using neutron fibre-diffraction patterns, which were obtained from DNA in H_2O and D_2O, have succeeded in illustrating the location of water molecules within ordered regions of A-DNA (Langan *et al.*, 1992; Shotton *et al.*, 1997), B-DNA (Shotton *et al.*, 1998) and D-DNA (Forsyth *et al.*, 1989; Fuller *et al.*, 1989). However, structural information at the atomic level could not be obtained owing to the limited resolution (see review by Fuller *et al.*, 2004). In this article, the structure of the Z-DNA hexamer d(CGCGCG) in heavy-water (D_2O) buffer is described. In particular, the hydration structure and the dynamic behaviour of the water molecules are discussed, as well as the unusual H/D exchange behaviour of the C8—H8 bonds of the guanine bases. This neutron structure determination was carried out at 1.8 Å resolution.

Table 1
Statistics of data collection and structure determination.

Values in parentheses are for the outer shell (1.66–1.60 Å for the neutron analysis and 1.45–1.40 the for X-ray analysis).

	Neutron	X-ray
Data collection		
Space group	$P2_12_12_1$	
Unit-cell parameters (Å)	a = 18.46, b = 30.76, c = 43.18	
Beam port (or radiation type)	1G, JRR-3M	Cu $K\alpha$
Wavelength (Å)	2.88 ($\Delta\lambda/\lambda$ = 0.015)	1.5418
Diffractometer	BIX-3	DIP-2000
Crystal size (mm^3)	1.6	1.4
Temperature (K)	298	293
Time (d)	70	3
Maximum resolution (Å)	1.6	1.4
Unique reflections	2627	4998
Redundancy	2.0 (1.7)	5.5 (5.4)
Completeness (%)	73.7 (40.9)	96.6 (96.1)
$I/\sigma(I)$	6.2 (3.5)	20.6 (12.6)
$R_{\rm merge}$ (%)	12.7 (20.8)	9.6 (19.7)
Refinement		
Resolution (Å)	25–1.8	10–1.5
R factor (%)	22.2	17.6
$R_{\rm free}$ (%)	29.4	21.0
R.m.s.d. bonds (Å)	0.005	0.003
R.m.s.d. angles (°)	0.83	0.80
Average coordinate error† (Å)	0.18	0.17
No. of non-H atoms	298	311
No. of H atoms	116	—
No. of D atoms	102	—
No. of D/H atoms	6	—
No. of water molecules	44	57
PDB code	1v9g	1woe

† Estimated from a Luzzati plot (Luzzati, 1952).

2. Materials and methods

2.1. Sample preparation and crystallization

The self-complementary DNA hexamer d(CGCGCG) was purchased from Qiagen KK. The crude oligonucleotide was purified by Sephadex-G10 gel filtration before crystallization. The purity of the DNA solution was assessed by a combination of UV spectroscopy and conductivity monitoring. The salt-impurity level in the crystallization solution was estimated to be lower than 0.1 m*M*, which was negligibly small. In order to avoid the high background arising from incoherent neutron scattering of H atoms, the crystallization was conducted in D_2O solution. Several crystallization conditions for the DNA hexamer d(CGCGCG) in H_2O have been reported previously (Dauter & Adamiak, 2001; Egli *et al.*, 1991; Gessner *et al.*, 1989; Wang *et al.*, 1979). These conditions were further refined in a D_2O buffer using a batch technique. In our case, the optimized conditions consist of 1.4 m*M* DNA with 100 m*M* sodium cacodylate pD 6.6, 30 m*M* spermine tetrahydrochloride, 30 m*M* magnesium chloride and 7.5% 2-methyl-2,4-pentanediol. Large crystals were obtained using the annealing technique. The largest crystal was grown in the following way: 1.0 ml of DNA solution containing the same components was prepared in a 2.0 ml microtube at 279 K. Numerous microcrystals appeared within a day. The tube was then placed into a 353 K heat block, the top of which was covered by several layers of aluminium foil in order to maintain a uniform temperature in the tube. This caused all the microcrystals in the tube to dissolve within 12 h. The DNA solution was then incubated at a lower temperature (338 K) for 24 h. Finally, the temperature of the heat block was systematically decreased from 338 to 298 K by 2 K per day. A few hexagonal plate-shaped crystals had appeared on the top of the DNA solution by the fifth day (328 K). As the temperature was systematically lowered, the crystals gradually increased in size and a 1.6 mm^3 crystal could finally be obtained.

2.2. X-ray analysis

In order to obtain the initial model for neutron structure determination, we solved the X-ray crystal structure of the Z-DNA hexamer grown from D_2O solution. The X-ray data were collected at 293 K using the oscillation method on a DIP-2000 diffractometer (MacScience Inc.) using Cu $K\alpha$ radiation and processed to 1.4 Å resolution using the programs *DENZO* and *SCALEPACK* (Otwinowski & Minor, 1997). The space group was determined to be $P2_12_12_1$, with unit-cell parameters a = 18.46, b = 30.76, c = 43.18 Å. A total of 4967 independent reflections were obtained with an overall $R_{\rm merge}$ of 9.8%. 4112 reflections from 10 to 1.5 Å resolution were used for structure determination. Initial phases were derived by the molecular-replacement method using the coordinates from the Z-DNA hexamer whose structure had been solved at the highest

resolution (0.6 Å) in X-ray crystallographic analysis of Z-DNA, obtained from H_2O solution (Tereshko *et al.*, 2001). The atomic parameters were refined with the program *CNS* (Brünger *et al.*, 1998). During the interpretation of the electron-density map with the program *XtalView* (McRee, 1999), an alternate conformation was found in the region of one phosphate group linking Gua8 and Cyt9 and was incorporated into the structure. 57 water molecules and one spermine molecule were included in the final model. The overall R factor was 17.6% (R_{free} = 21.0%). The statistics of the X-ray experiment and data collection and structure determination are summarized in Table 1.

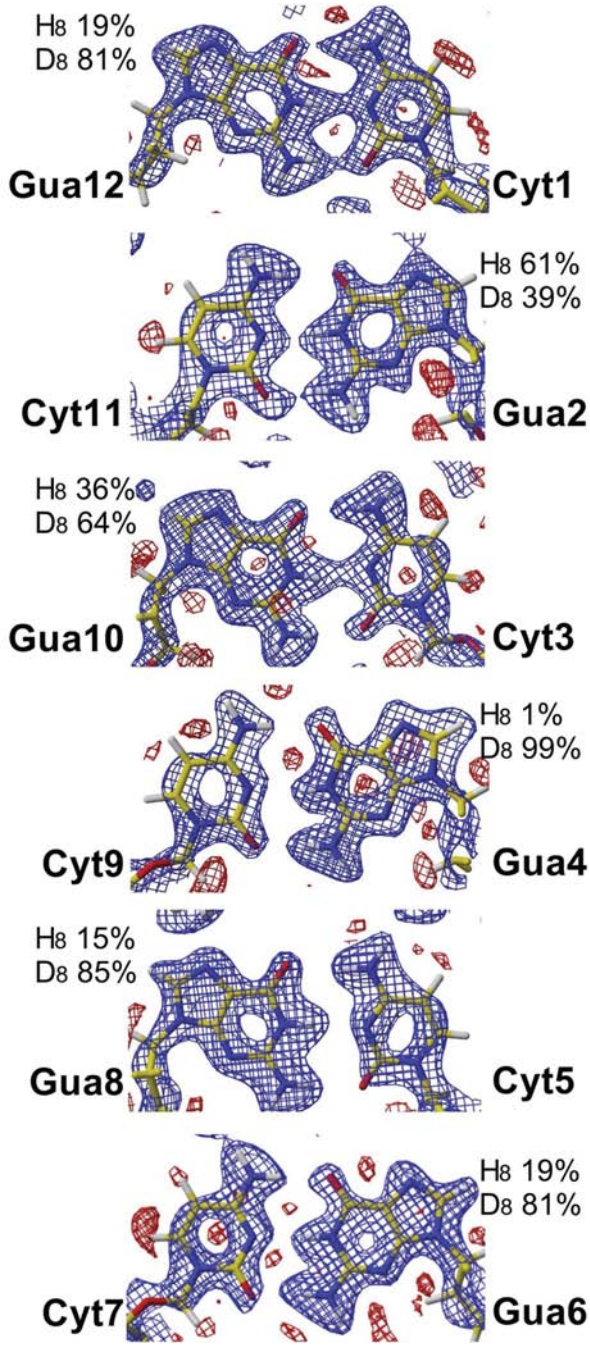

Figure 1
Final refined $2|F_o| - |F_c|$ neutron Fourier map superimposed on the G–C skeletons of the Z-DNA hexamer d(CGCGCG). The blue and red contours show positive (1.5σ) and negative densities (-2.5σ), respectively. Note that positive contours are found near almost all of the C8 atoms of the purine rings (except Gua2), showing evidence of C8—H/C8—D exchange and hence demonstrating the unusual acidity of the H8 proton of guanine.

2.3. Neutron analysis

Neutron diffraction data were collected with the BIX-3 instrument in reactor JRR-3M at JAERI (Tanaka *et al.*, 2002). The neutron beam size is φ = 5 mm and its wavelength is 2.88 Å ($\Delta\lambda/\lambda$ = 0.015). A step-scan data-collection method with an interval of 0.3° between frames was used. The diffraction patterns were processed to 1.6 Å resolution using the programs *DENZO* and *SCALEPACK* (Otwinowski & Minor, 1997), specially modified for BIX-3 (Atec Corp.) in order to increase the efficiency of the integration process. 2627 independent reflections were obtained with an overall R_{merge} of 12.7%. Phase determination and structure refinement were performed with the program *CNS* (Brünger *et al.*, 1998). All density-map visualizations and interpretations were performed using the program *XtalView* (McRee, 1999). The initial model was derived from the X-ray structure. H and D atoms in Z-DNA (36 D and 96 H atoms) and spermine (10 D and 20 H) were initially placed at stereochemically calculated positions except the four D atoms of the —OD functional groups at the 5′- and 3′-termini. Those D atoms were placed at locations revealed by a neutron $2|F_o| - |F_c|$ Fourier map. Positive contours higher than the 3σ level in a neutron $|F_o| - |F_c|$ Fourier map were considered as candidates for D_2O molecules by analyzing the hydrogen-bond patterns around them and also by comparing their locations with the oxygen positions as obtained in the X-ray structure determination. 44 of the 57 D_2O molecules identified from the X-ray structure determination were included into the neutron structure. Several D_2O molecules lacked portions of their nuclear densities because of disorder. While 29 of the 44 D_2O molecules modelled in the neutron structure contained the entire contour of three atoms (D—O—D), 15 D_2O molecules only had a simple spherical contour corresponding either to a single O atom or the gravitational centre of a completely rotationally disordered D_2O molecule. The remaining 13 D_2O molecules found in the X-ray structure had diffuse contours lower than 3σ level in the neutron maps and these were considered to be unobserved. Finally, the occupancies of the D atoms of the C8—H8 bonds of the guanine bases were refined. The statistics of the neutron experiment are summarized in Table 1.

3. Results and discussions

3.1. H and D atoms in the nucleic acid bases and in the spermine cation

Almost all the D and H atoms in the Z-DNA molecule were observed, as shown in Fig. 1. Red contours indicate negative densities (-2.5σ) corresponding to the H atoms of most of the C—H bonds, while blue contours correspond to positive regions ($+1.5\sigma$) such as the D atoms of N—D bonds. Polar H

atoms (such as those of most N—H and O—H bonds) can be exchanged by D atoms because the Z-DNA crystal was grown from D_2O buffer. In contrast, H atoms bonded to carbon are normally not exchangeable. An exception is the H atom bonded to the C8 atom of the guanine (Gua) base, which has some acidic properties. Therefore, this H atom is in principle exchangeable with D atoms from the solvent. Fig. 1 indicates the direct experimental evidence for this in the d(CGCGCG) hexameric duplex. Almost all the guanine bases show evidence of a substantial amount of H/D exchange. An average of 75% of the H8 atoms are estimated to have been replaced by D atoms. Only the H8 atom of Gua2 did not exhibit a positive contour, indicating low deuterium occupancy at that position and suggesting that the H8/D8-exchange ratio may depend on the environment of a particular C8—H8 bond. H8 atoms in three of the six guanine bases (Gua4, Gua6 and Gua8) are within 3 Å of negatively charged O atoms of phosphate groups in the neighbouring duplex (Fig. 2*a*). The interaction between the H8 atom and the phosphate group increases the acidity of the C8—H8 bond (Egli & Gessner, 1995). It is thought that the nucleophilic interaction of the O atom, which has a lone pair of electrons, with the C8—H8 bond provokes deprotonation of this C—H bond. Another H8 atom in Gua12 makes a C8—H8$\cdots$O4′ hydrogen bond with the O4′ atom of Gua2, causing an electrostatic effect similar to that of the phosphate group (Fig. 2*b*). Consequently, the populations of D atoms at these four positions are above 80%. On the other hand, the two remaining H8 atoms (Gua2 and Gua10), which only contact a D_2O molecule or make no contacts (Fig. 2*c*), have lower H8/D8-exchange ratios. They are summarized in Table 2.

Previous proton NMR studies suggested that the H8/D8-exchange ratio is positively correlated with temperature and that in particular the transition from the B to the Z conformation enhances the H/D exchange greatly (Brandes & Ehrenberg, 1986). The temperature of the present crystallization (T = 353–298 K) and the helical conformation of the DNA duplex (Z-form) are thus favourable parameters for H8/D8 exchange. It has long been known that the C8—H8 group has a chemical reactivity that is higher than those of other C—H bonds in nucleic acids. For example, active oxygen species react with guanine bases in DNA and dNTP pools to form C8-oxidized guanines (Fuciarelli *et al.*, 1990; Park *et al.*, 1992), which cause G–T transversions *in vivo* (Wood *et al.*, 1990). Thus, H8/D8-exchange information can be useful in helping us understand some mechanisms of mutagenesis.

Incidentally, the $C^{\varepsilon 1}$—H of the imidazole group in histidine residues of proteins is the most acidic C—H bond found in amino acids (Matsuo *et al.*, 1972). This C—H bond is similar to the C8—H8 bond of guanine since both are located between

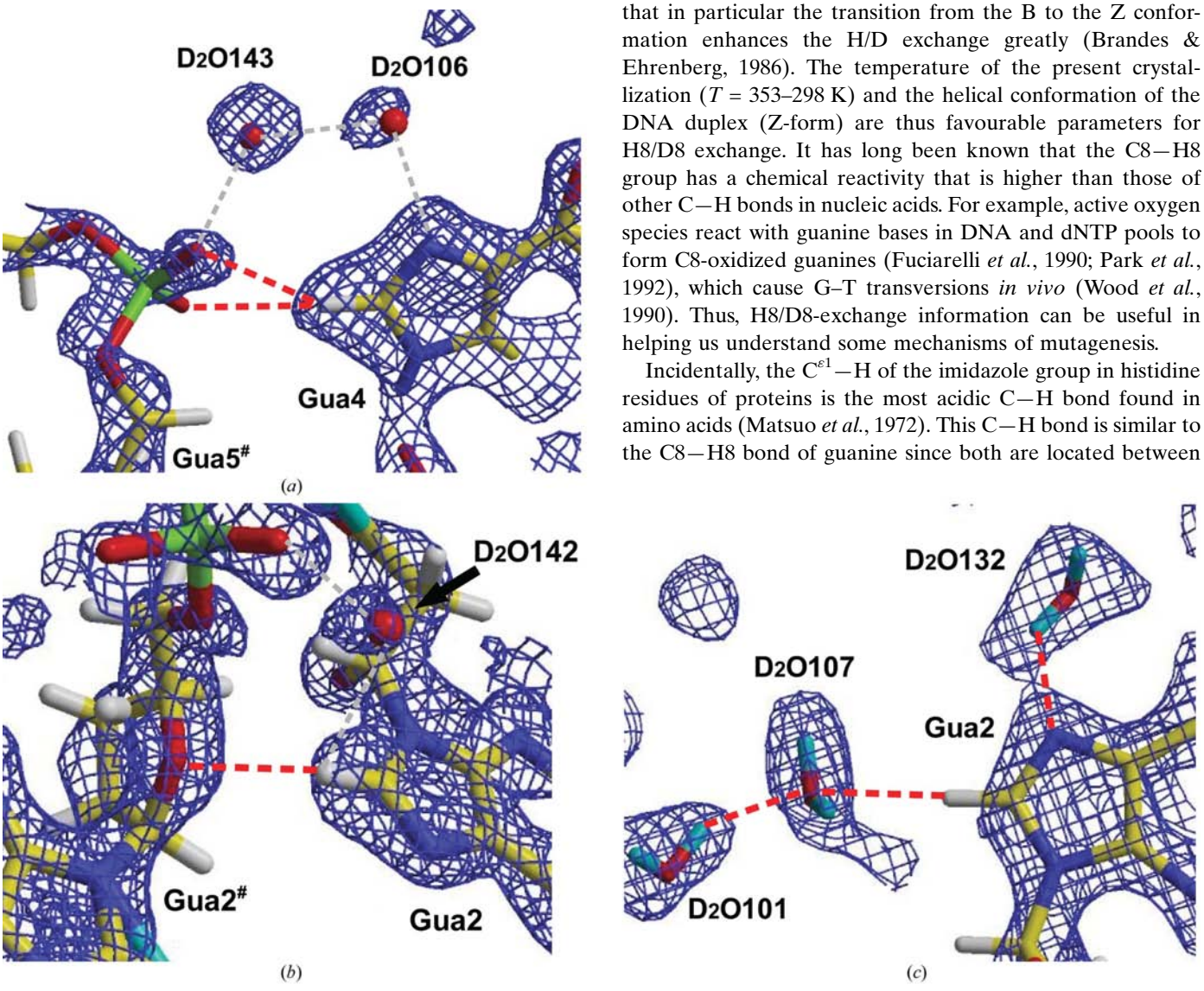

Figure 2
C8—H8 bonds in guanine bases interacting with (*a*) the phosphate group in the neighbouring Z-DNA duplex, (*b*) the O atom in a ribose ring of the symmetry-related oligonucleotide and (*c*) a D_2O molecule. The blue contours show positive (1.5σ) densities in the $2|F_o| - |F_c|$ Fourier map. Red and grey broken lines show the location of actual and possible hydrogen bonds, respectively. The C8—H8 bonds near the negative charged atom in (*a*) and (*b*) have been considerably deuterated, while the H8/D8-exchange ratio in the C8—H8 bonds surrounding D_2O molecules is low (*c*).

Table 2
The interaction of C8—H8 bonds with Z-DNA and D_2O molecules.

Atom	Percentage D	Acceptor atom in Z-DNA and D_2O		Distance (Å)	Angle (°)	Symmetry operation
H8/D8 in Gua2	39	O	D_2O107	2.43	158.2	
H8/D8 in Gua4	99	O1P	Cyt5	2.71	152.3	$(x + 1/2, -y + 3/2, -z + 1)$
		O2P	Cyt5	2.88	145.0	$(x + 1/2, -y + 3/2, -z + 1)$
		O	D_2O104	2.88	145.0	
H8/D8 in Gua6	81	O1P	Cyt3	2.85	123.0	$(x - 1/2, -y + 3/2, -z + 1)$
H8/D8 in Gua8	81	O2P	Cyt3	2.37	108.5	$(x + 1/2, -y + 1/2, -z + 1)$
H8/D8 in Gua10	64					
H8/D8 in Gua12	85	O4′	Gua2	2.67	131.2	$(x - 1, y, z)$

two N atoms in a five-membered ring. We have also recently confirmed H/D exchange of the $C^{\varepsilon 1}$—H bond of histidine in metmyoglobin (Ostermann *et al.*, 2002), hen egg-white lysozyme (Bon *et al.*, 1999) and insulin (Maeda *et al.*, 2004) by the neutron diffraction technique. It is therefore expected that H/D exchange of acidic C—H bonds would frequently occur in certain biomolecules when exposed to D_2O.

Also found is one positively charged spermine cation (SPM^{4+}), the chemical formula of which is $[ND_3(CH_2)_3ND_2(CH_2)_4ND_2(CH_2)_3ND_3]^{4+}$, bound to the phosphate groups and the major groove of the Z-DNA. The interactions of SPM^{4+} with Z-DNA and water molecules are shown in Table 3. The $-ND_3^+$ and $-ND_2^+$ groups in SPM^{4+} neutralize the negative charges of the phosphate groups. In addition, the SPM^{4+} cation links three symmetry-related Z-DNA duplexes by salt bridges and thus seems to be indispensable to crystal packing.

3.2. Present crystal form of the Z-DNA

Various crystal forms of d(CGCGCG) could be obtained from DNA solution containing different components (Malinina *et al.*, 1991). Although the crystals belong to the same space group $P2_12_12_1$, three basic crystal forms of this DNA hexamer were analyzed and included either $MgCl_2$ and spermine (Mg-Spr crystal; Wang *et al.*, 1979; PDB code 2dcg), $MgCl_2$ only (Mg crystal; Gessner *et al.*, 1989; PDB code 1dcg) or spermine only (Spr crystal; Bancroft *et al.*, 1994; Egli *et al.*, 1991; PDB code 1d48). Although the present crystal was obtained from solutions including $MgCl_2$ and spermine, its helical structure bore a close resemblance to that of the Spr form. Its root-mean-square differences in atomic positions from those in Mg-Spr, Mg and Spr crystals are 0.90, 0.78 and 0.67 Å, respectively. Moreover, it has a characteristic feature of the Spr crystal: an alternate conformation of one phosphate group linking Gua8 and Cyt9. As shown in Fig. 3, the X-ray map illustrates two distinguishable conformations in the present crystal. In the cases of the Mg and Mg-Spr crystals, the corresponding backbone only took conformation 1 in Fig. 3, while both the conformations were partially occupied in the Spr crystal. 70% of the water molecules were also conserved between the Spr and the present crystals. Positional differences between the oxygen positions of corresponding water molecules are less than 0.5 Å after superimposing the two structures.

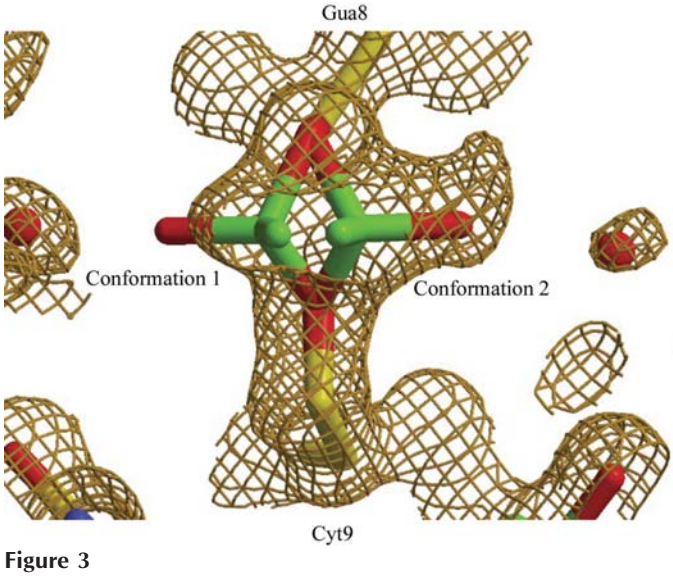

Figure 3
Alternate conformations of a phosphate group linking Gua8 and Cyt9 residues. An X-ray $2|F_o| - |F_c|$ Fourier map is superimposed on the model ($+1.5\sigma$).

Nevertheless, the Spr crystal and the present crystal have entirely different chemical compositions. Two SPM^{4+} cations were contained in the Spr crystal. One of these is tightly bound to Z-DNA and was clearly observed by X-ray analysis at room temperature (Egli *et al.*, 1991). Another has higher *B* factors and low-temperature X-ray analysis was necessary to find it (Bancroft *et al.*, 1994). In contrast, the present crystal only includes the former SPM^{4+}. The latter SPM^{4+} was replaced with a row of four ordered water molecules as shown in Fig. 4. It is interesting to consider why such differences arise. In our experience of crystallizations using D_2O solution (Chatake, Mizuno *et al.*, 2003, Chatake *et al.*, 2004), the deuterated environment does not significantly affect the crystal structure. It is plausible that the present structural changes were mainly derived from the high temperature (T = 353–298 K) during crystallization. It is thought that there is a low energy barrier between the two conformers in the backbone linking Gua8-Cyt9 and that Z-DNA cannot tightly fasten SPM^{4+} in the second binding site. It is concluded that the present crystal is a new form, reflecting the high-temperature structure of the Z-DNA.

3.3. Water structure

Two types of water molecule have been found in the hydration shells around the present Z-DNA, as shown in Fig. 5.

Table 3
The interaction of the spermine cation (SPM^{4+}) with Z-DNA and D_2O molecules.

D atom in SPM^{4+}	Acceptor atom in Z-DNA and D_2O		Distance (Å)	Angle (°)	Symmetry operation
1D1	O	D_2O104	2.63	132.7	
1D1	O1P	Cyt3	2.40	132.0	(x, y, z)
2D1	O1P	Gua12	2.52	96.8	$(x + 1, y, z)$
3D1	O1P	Gua12	2.29	111.6	$(x + 1, y, z)$
3D1	O5′	Gua12	2.35	176.1	$(x + 1, y, z)$
1D5	O1P	Cyt11	2.85	123.0	$(x + 1, y, z)$
1D5	O2P	Cyt11	2.09	176.5	$(x + 1, y, z)$
2D5	O	D_2O104	2.10	144.6	
1D10	N7	Gua8	1.97	109.6	(x, y, z)
2D10	O2P†	Cyt9	1.90	149.8	$(x + 1/2, -y + 1/2, -z + 1)$
2D10	O1P†	Cyt9	2.44	127.1	$(x + 1/2, -y + 1/2, -z + 1)$
2D10	O1P‡	Cyt9	2.47	145.2	$(x + 1/2, -y + 1/2, -z + 1)$
1D14	O	D_2O135	2.33	117.5	
1D14	N7	Gua10	2.51	102.8	$(x + 1/2, -y + 1/2, -z + 1)$
2D14	N7	Gua10	2.48	104.7	$(x + 1/2, -y + 1/2, -z + 1)$
2D14	O6	Gua10	2.28	154.5	$(x + 1/2, -y + 1/2, -z + 1)$
2D14	O	D_2O136	2.68	124.3	
3D14	O6	Gua2	2.92	121.6	$(x + 1/2, -y + 1/2, -z + 1)$

† Atoms in conformation *A* in the coordinate file. ‡ Atom in an alternate conformation *B*.

In some cases in the present neutron structure a complete water molecule (one O and two D atoms) can be clearly identified as a triangular contour in the neutron Fourier map, while a spherical contour corresponds to the centre of gravity of a water molecule that is rotationally disordered. A total of 29 ordered and 15 rotationally disordered D_2O molecules could be observed in the neutron structure. The appearances of water molecules seem to be related to their dynamic behaviour. Small and large *B* factors obtained from the X-ray analysis correspond to D_2O molecules having triangular and spherical contours in the neutron Fourier maps, respectively. Triangular-shaped D_2O molecules have an average *B* factor of 25.9 $Å^2$, while spherical-shaped D_2O molecules have an average *B* factor of 31.1 $Å^2$. This tendency, in which the *B* factors of an X-ray structure determination are positively correlated with the shapes of contours in a neutron structure, has been noticed previously (Teeter & Kossiakoff, 1984; Chatake, Ostermann *et al.*, 2003).

It is interesting to determine whether there is any correlation between the shape of a water molecule and its location in hydration shells. Generally, the surface of the Z-DNA could be divided into three regions: a major groove, a minor groove and a phosphate backbone. Unfortunately, no D_2O molecules in the second hydration shell of the Z-DNA could be assigned in the neutron analysis, because of the small crystal lattice (2.45×10^5 $Å^3$) and the lower resolution and high temperature of our neutron structure determination compared with earlier X-ray analyses. The distribution of D_2O molecules (*i.e.* numbers of waters located, shapes, *B* factors) associated with the three kinds of surface region are shown in Table 4. Totals of 12, 13 and 19 D_2O molecules have been located around the minor groove, the major groove and the phosphate backbone, respectively. Most of the D_2O molecules in the minor groove (11 out of 12) have triangular contours corresponding to ordered water molecules, while only half of the D_2O molecules in the major groove have this appearance. This means that the dynamic behaviour of water molecules appears to depend on their locations; in other words, the water molecules in the major groove seem to be more dynamic (more disordered) than those in the minor groove. This tendency seems reasonable because it is thought that the water molecules in the minor groove are used as the main framework for DNA folding and are tightly bound to B-DNA and Z-DNA (Drew & Dickerson, 1981; Wang *et al.*, 1979).

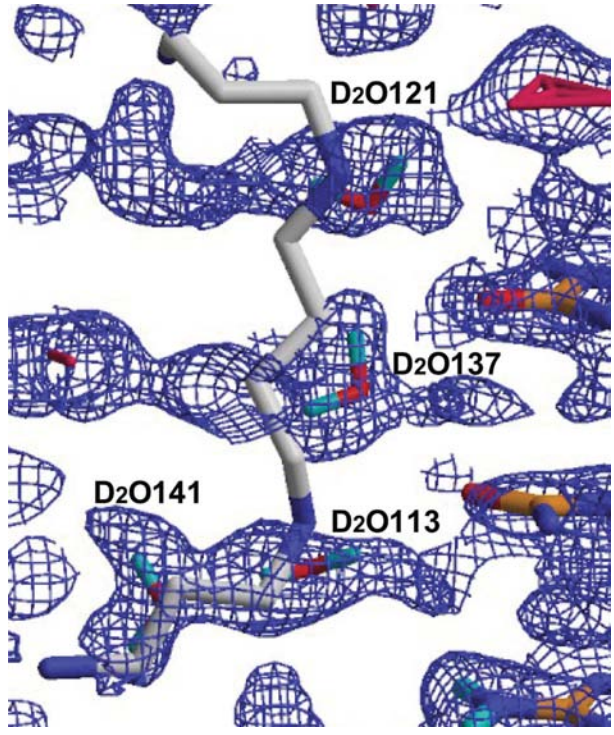

Figure 4
A neutron $2|F_o| - |F_c|$ Fourier map in the region where the second spermine molecule was observed in the minor groove of the Z-DNA in the pure spermine form (Spr crystal). The spermine molecule (drawn as a zigzag stick model) was replaced with four D_2O molecules (D_2O113, D_2O121, D_2O137 and D_2O141) in the present crystal.

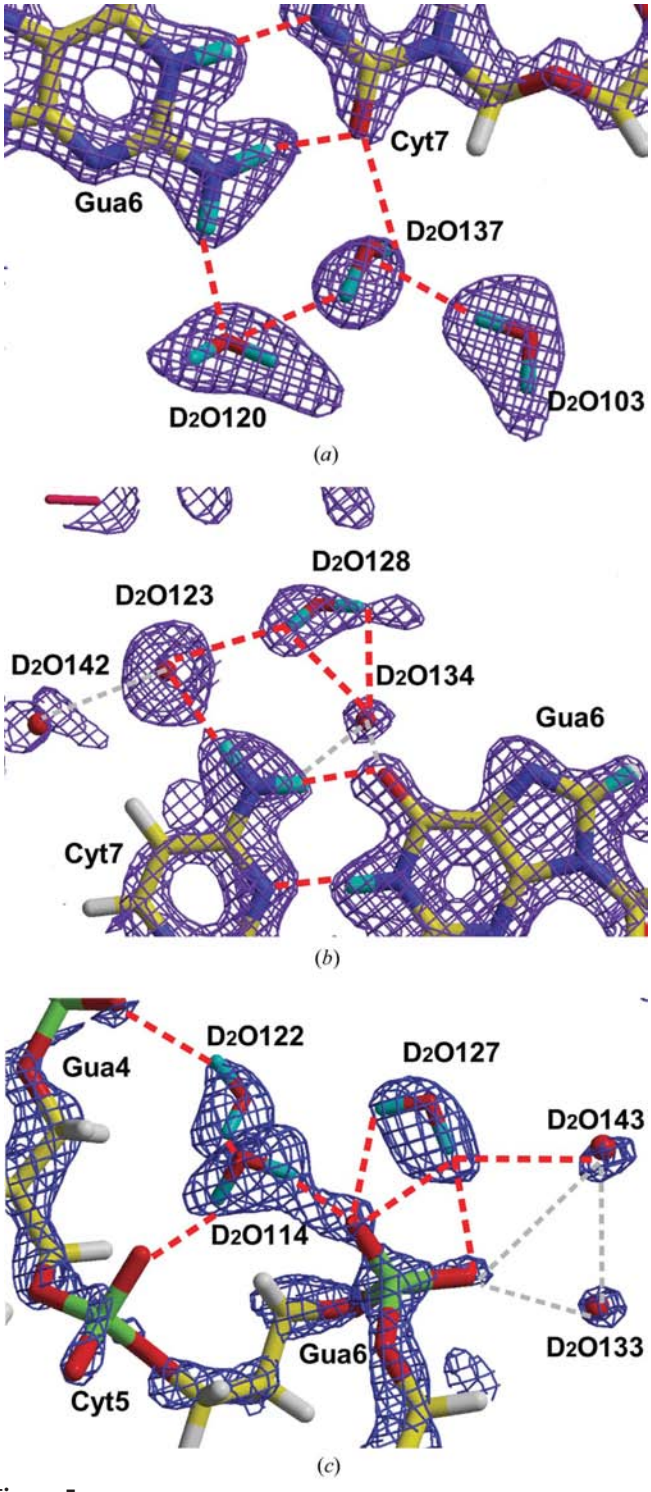

Figure 5
Typical examples of water molecules on the surface of the Z-DNA hexamer (*a*) in the minor groove, (*b*) in the major groove and (*c*) around the phosphate backbone. Two appearances of water molecules were observed in the neutron $2|F_o| - |F_c|$ Fourier maps. Triangular-shaped contours indicate ordered D_2O molecules in which all atoms (one O and two D) could be observed. In contrast, spherical-shaped contours show rotationally disordered D_2O molecules and in this case only the centre of gravity of the water is observed. Red and grey broken lines show the location of actual and possible hydrogen bonds, respectively. Spherical contours (*i.e.* disordered water molecules) were frequently observed in the major groove (Fig. 5*b*) and around the phosphate backbone (Fig. 5*c*), but not in the minor groove (Fig. 5*a*).

Table 4
Statistics of D_2O molecules from the neutron analysis of Z-DNA.

'Triangular' water molecules are those in which all three atoms (D, O, D) were located in the neutron density map. 'Spherical' water molecules are those that are rotationally disordered in the neutron density map. 'Missing' waters are those found in the X-ray analysis but not found in the neutron analysis.

Classification	Triangular	Spherical	Missing
Number	29	15	13
Average *B* factor (Å^2)			
Neutron	19.3	51.0	
X-ray	25.9	31.1	35.8
Location			
Minor groove	11	1	0
Major groove	8	5	2
Others	10	9	11

3.4. Possible Na^+ and Mg^{2+} atoms in the structure

13 D_2O molecules found near the phosphates of Z-DNA in the X-ray analysis had contours lower than the 3σ level in the neutron Fourier map. Some of them may not be D_2O molecules but could be metal ions (Mg^{2+} or Na^+ cations). The Z-DNA duplex has a total of ten negative charges from the phosphate groups, but only four positive charges in the spermine ion could be accounted for in the neutron analysis. The remaining six positive charges should be in the crystal as monovalent or divalent cations. In the X-ray analysis, it is difficult to distinguish between D_2O, Na^+ and Mg^{2+} without precise measurement of anomalous scattering (Tereshko *et al.*, 2001), because their X-ray scattering factors are almost the same (about 10 e^-). On the other hand, the neutron scattering lengths of Na^+ (3.6 fm) and Mg^{2+} (5.4 fm) are much smaller than the three-atom combination of D_2O (19.1 fm). Therefore, these cations have very low contours in a neutron Fourier map. The D_2O molecules labelled 126, 127, 130, 144 145, 146 and 150 in our X-ray structure (PDB code 1woe) are suspected to be candidates for Na^+ or Mg^{2+} ions because of their proximity to the negatively charged phosphate groups of the backbone. However, those peaks are lower than the 1.0σ level in our neutron $2|F_o| - |F_c|$ Fourier map and hence any conclusive identification of them as Na^+, Mg^{2+} or disordered D_2O molecules is not possible from the neutron data. In particular, D_2O130 is located in the position corresponding to the Mg^{2+} cation in the spermine/magnesium mixed crystal (PDB code 2dcg). As shown in Fig. 6(*a*), the Mg^{2+} cation binds at the N^7 position of Gua6 by direct coordination and has an octahedral hydration shell with ion–water distances of 2.1–2.3 Å. However, the regular coordination could not be observed around D_2O130 (Fig. 6*b*).

3.5. Hydrogen-bonding networks

In the present study, the definition of a hydrogen bond is that the distance between proton and proton acceptor is shorter than 2.8 Å and the angle (X—D$\cdots Y$, where X is the proton donor and Y the proton acceptor) is greater than 90°. As shown in Fig. 5, many hydrogen bonds were found in the solvent region. The three-dimensional hydrogen-bonding network, including D atoms observed by the present neutron

analysis, is complicated. A typical example showing this complexity is illustrated in Fig. 7. In the minor groove of the Z-DNA, although the O atoms of the water molecules are located on a straight line, the orientations of the water molecules are not the same. Consequently, the hydrogen-bonding network is quite complicated. Very recently, we have solved the neutron structure of the B-DNA decamer d(CCATTAATGG) at 3.0 Å resolution (Arai *et al.*, 2005), in which the hydrogen-bonding network is also complicated, as in the present Z-DNA. This coincides with the present observation.

Previously, the three X-ray crystal structures (Mg-Spr, Mg and Spr crystals) mentioned in §3.2 have been compared and several common locations of water molecules (positions of O atoms) have been found in the first hydration shell of Z-DNA (Gessner *et al.*, 1994). D_2O molecules observed by the present analysis could also be categorized in a similar manner. The hydrogen-bonding patterns of D_2O molecules depending on their location will be described in the following sections.

3.5.1. Hydrogen-bonding networks in the minor groove of the Z-DNA. Two types of regular hydrogen-bonding patterns could be observed in the minor groove of Z-DNA.

(i) An N2 amino group of a guanine base and a phosphate group in the same chain are bridged by an indirect hydrogen-bonding network mediated by one or two D_2O molecules. Every binding site of N2 position was occupied by a triangular-shaped D_2O molecule, implying their contribution in building the Z-DNA structure. A typical example of this interaction has two hydrogen-bonding routes as shown in Fig. 8. The O atom from D_2O122 and the N2 1D2 group from Gua4 make a hydrogen bond, while the one-dimensional atom from D_2O122 is hydrogen bonded to the O2P atom from Gua4 and makes a weak hydrogen bond to the O3′ atom of Cyt3, respectively. In addition, the D2 atom (D_2O122) is hydrogen bonded to the O atom from D_2O114, of which the D1 and D2 atoms form

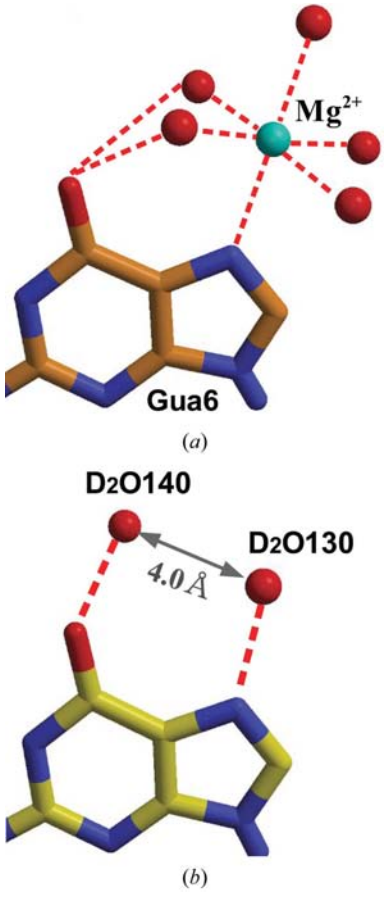

Figure 6
A diagram showing (*a*) Mg^{2+} coordination geometry at the N7 position with an octahedral hydration shell observed in the magnesium/spermine mixed crystal (PDB code 2dcg) and (*b*) the D_2O130 molecules at the corresponding position in the present crystal.

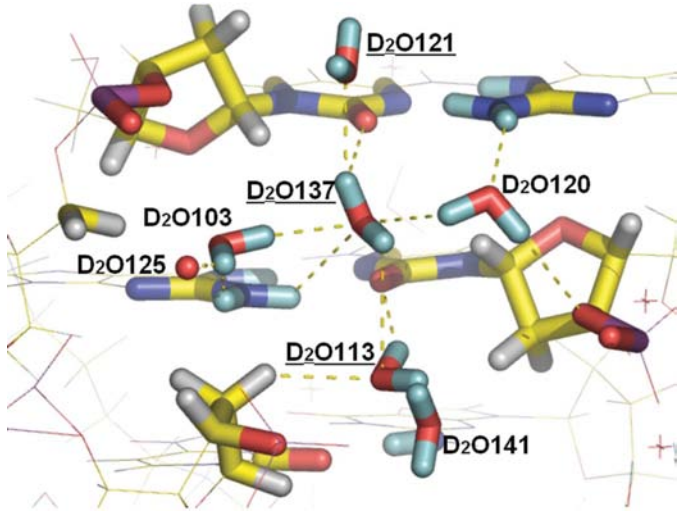

Figure 7
A schematic diagram showing the complicated hydration structure in the minor groove between the Gua4–Cyt9 and Gua6–Cyt7 base pairs. The three D_2O molecules with underlined labels (D_2O121, D_2O137 and D_2O113) are located at the bottom of the minor groove. This diagram includes all covalent bonds within a radius of 7 Å from the O atom of D_2O137. Yellow broken lines show hydrogen bonds.

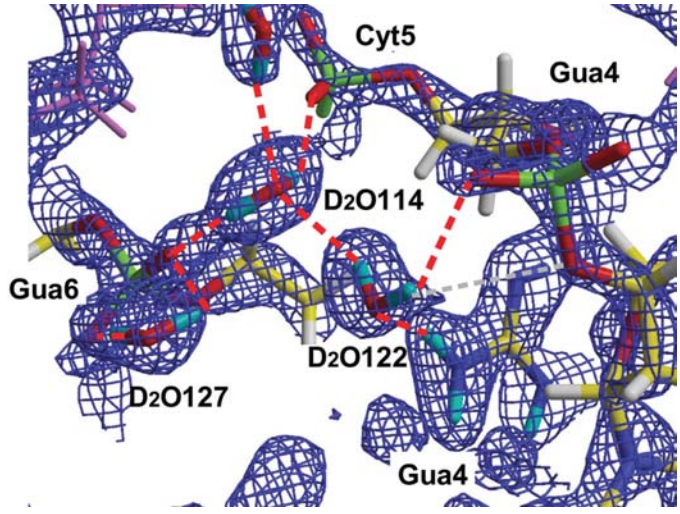

Figure 8
A neutron $2|F_o| - |F_c|$ Fourier map around the hydrogen-bonding network linking the N2 amino group (Gua4) and the phosphate backbone. Red and grey broken lines show hydrogen bonds and electrostatic interactions weaker than hydrogen bonds defined in this manuscript.

hydrogen bonds with the O1P atom from Gua6 and the O2P atom from Cyt5, respectively. We summarize the details of these interactions in Fig. 9(*a*). The branching hydrogen-bonding network could be observed in Gua4 and Gua6. In the remaining cases only hydrogen-bonding networks mediated by one D_2O molecule could be observed, except for Gua8, where the water bridge was broken because of the alternate conformation mentioned in §3.2.

(ii) Another hydrogen-bonding pattern could be found between cytosine N4 amino groups. As shown in Fig. 9(*b*), the hydrogen-bonding scheme differs between the upper and the lower solvent regions. In the upper region (D_2O118, D_2O111 and D_2O124), two D atoms in the D_2O molecule form hydrogen bonds or electrostatic interactions with two O2 groups in neighbouring cytosine bases. This hydrogen-bonding scheme is very similar to the interaction pattern proposed by previous X-ray analyses (Gessner *et al.*, 1994). In contrast, a different hydrogen-bonding pattern was observed in the lower region (D_2O113, D_2O137 and D_2O121). Each D_2O molecule is hydrogen bonded to only one cytosine base and they are connected to each other by hydrogen bonding. This solvent region corresponds to the area occupied by the second spermine molecule in the Spr crystal. It has been reported that in

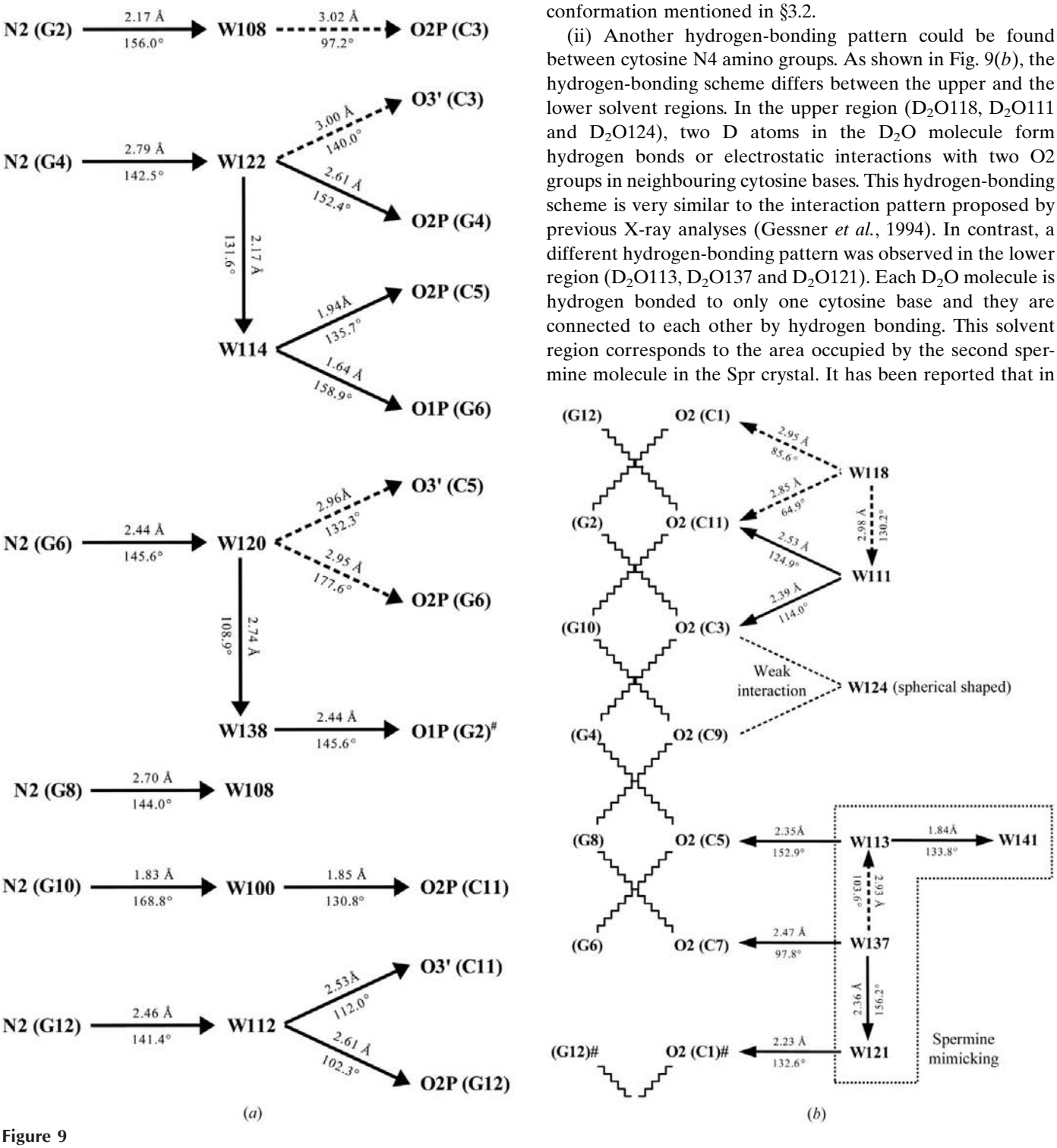

Figure 9
A schematic diagram of the hydrogen-bonding networks in the minor groove of the Z-DNA hexamer. (*a*) Hydrogen bonds bridging N2 amino groups from guanine bases and phosphate groups in the backbone. Arrows show the directions of the hydrogen bonds (from proton donor to acceptor). Broken lines are electrostatic interactions weaker than the hydrogen bond defined in the text. A symmetry-related atom is marked #. (*b*) Hydrogen bonds bridging O2 keto groups from cytosine bases. Wavy lines represent the connection of the Z-DNA duplex. D_2O124 has a spherical contour in the neutron $2|F_o| - |F_c|$ Fourier map; therefore, the interaction between this D_2O molecule and Z-DNA was ambiguously observed. Note that the hydrogen-bonding scheme in the lower region differs from that in the upper region because the D_2O113, D_2O137, D_2O121 and D_2O141 molecules mimic the second spermine molecule in the Spr crystal (containing two spermine molecules) as shown in Fig. 4.

the Mg^{2+}-free B-DNA crystals, a five-membered ring of water molecules occupies the same position as a hydrated Mg^{2+} site (Tsunoda *et al.*, 2001). It is suggested that the three D_2O molecules make this particular interaction in order to mimic the spermine molecule with an additional D_2O141 molecule. It can be concluded that the hydrogen-bonding networks in the minor groove have some flexibility as well as periodicity and regularity as expected from X-ray crystallography.

3.5.2. Hydrogen-bonding networks in the major groove and the phosphate backbone. There are three binding sites for D_2O molecules in each d(C–G) pair: the O6 and N7 atoms from the guanine base and the N4 atom from the cytosine base. Only hydration at the N7 positions could clearly be observed as shown in Fig. 10(*a*), where two D_2O molecules link two N7 amino groups from a neighbouring cytosine. In contrast, the hydrogen-bonding networks anchored at the other positions (O6 or N7 atoms) could hardly be observed (Fig. 10*b*). The major groove of Z-DNA is shallower than those of the other forms of DNA, suggesting difficulty in making rigid hydrogen-bonding networks on its convex surface. The average *B* factor of D_2O molecules in the major groove (28.0 $Å^2$) is higher than for those the minor groove (21.3 $Å^2$), supporting this assumption. It could be speculated that the hydrogen-bonding networks in the minor groove are involved in the main structural framework in DNA, while the hydrogen-bonding networks in the major groove are used to transmit the genetic information recorded on DNA. It is thought that the hydrogen-bonding differences between the two grooves are derived from their function.

The tendency for rotational disorder of D_2O molecules is very high around phosphate groups (Fig. 5*c*). Therefore, no systematic hydrogen-bonding network could be found in this area, except for the N2 (Gua)—D_2O—P interaction (as described in §3.5.1) or crystal packing.

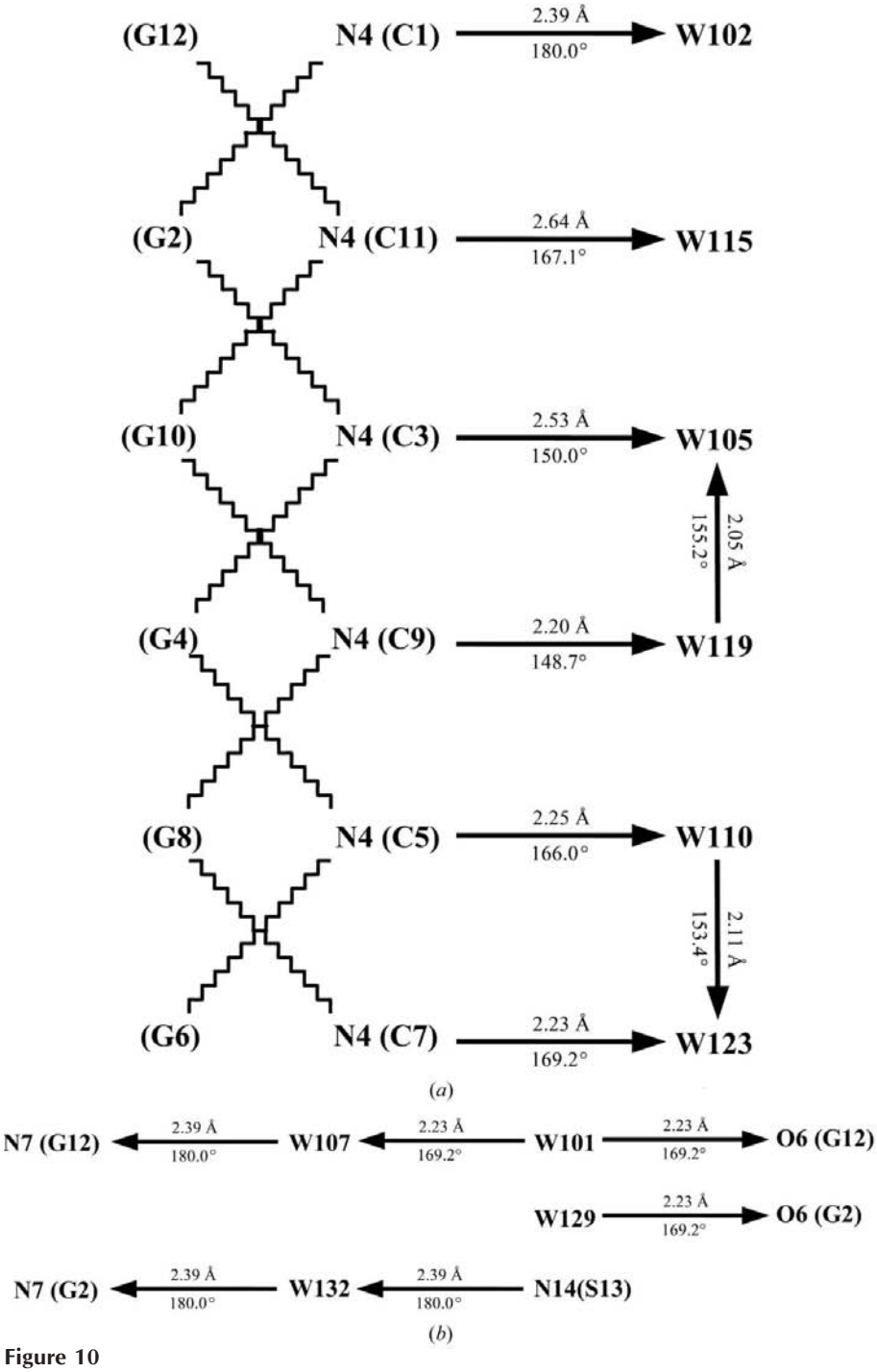

Figure 10
A schematic diagram of the hydrogen-bonding networks in the major groove. (*a*) Hydrogen bonds bridging N4 amino groups from cytosine bases in the major groove of the Z-DNA. D_2O115 and D_2O123 have spherical contours in a neutron Fourier map. (*b*) Other hydrogen bonds in the major groove coordinated at the N7 or O6 atoms of guanine bases.

4. Conclusion

In the present neutron crystallographic analysis at 1.8 Å, almost all positions of the H and D atoms of the Z-DNA hexamer could be located and refined. In particular, the C8—H8 groups of the guanine bases took part in H/D exchange because of the acidic properties of these C—H bonds. The H8/D8-exchange ratio depends on the environment of a particular C8—H8 bond. In the solvent region, 44 D_2O molecules were found from the nuclear density maps. They could be categorized into two classes according to the tendency for disorder: 29 D_2O molecules were well ordered, while the remaining 15 D_2O molecules were rotationally disordered. In the minor groove almost all

D_2O molecules were well ordered, while the disordered D_2O molecules were frequently observed in the major groove. This suggests that the dynamic behaviour of the hydration structure differs between the minor- and major-groove regions. The hydrogen-bonding networks including H (D) atoms could be observed in the solvent region. As well as the dynamic behaviour of D_2O molecules, the formation of a hydrogen bond depends on its location. Moreover, even the well ordered hydration in the minor groove has a certain amount of fluctuation.

It can be concluded that the hydrogen-bonding and hydration structure of Z-DNA observed by neutron diffraction study can provide new insights for discussion of DNA folding and dynamics. We have found several different types of dynamic behaviour of water molecules depending on their locations and the fluctuation of the hydrogen-bonding network. They may contribute to the flexibility of the DNA helix and may facilitate conformational changes such as the B-to-Z transition.

We are grateful to Dr Satoru Fujiwara and Professor Gen Sazaki for discussions concerning DNA crystallization. We thank Professor Robert Bau for valuable suggestions and assistance in refining the expression of this manuscript. This work was supported in part by an 'Organized Research Combination System' Grant from the Ministry of Education, Culture, Sports, Science and Technology of Japan.

References

Arai, S., Chatake, T., Ohhara, T., Kurihara, K., Tanaka, I., Suzuki, N., Fujimoto, Z., Mizuno, H. & Niimura, N. (2005). In preparation.
Bancroft, D., Willian, L. D., Rich, A. & Egli, M. (1994). *Biochemistry*, **33**, 1073–1086.
Behe, M. & Felsenfeld, G. (1981). *Proc. Natl Acad. Sci. USA*, **78**, 1619–1623.
Bon, C., Lehmann, M. S. & Wilkinson, C. (1999). *Acta Cryst.* D**55**, 978–987.
Brandes, R. & Ehrenberg, A. (1986). *Nucleic Acids Res.* **14**, 9491–9508.
Brünger, A. T., Adams, P. D., Clore, G. M., DeLano, W. L., Gros, P., Grosse-Kunstleve, R. W., Jiang, J.-S., Kuszewski, J., Nilges, N., Pannu, N. S., Read, R. J., Rice, L. M., Simonson, T. & Warren, G. L. (1998). *Acta Cryst.* D**54**, 905–921.
Chatake, T., Kurihara, K., Tanaka, I., Tsyba, I., Bau, R., Jenney, F. E. Jr, Adams, M. W. & Niimura, N. (2004). *Acta Cryst.* D**60**, 1364–1373.
Chatake, T., Mizuno, N., Voordouw, G., Higuchi, Y., Arai, S., Tanaka, I. & Niimura, N. (2003). *Acta Cryst.* D**59**, 2306–2309.
Chatake, T., Ostermann, A., Kurihara, K., Parak, F. G. & Niimura, N. (2003). *Proteins*, **50**, 516–523.
Dauter, Z. & Adamiak, D. A. (2001). *Acta Cryst.* D**57**, 990–995.
Dickerson, R. E., Drew, H. R., Conner, B. N., Wing, R. M., Fratini, A. V. & Kopka, M. L. (1982). *Science*, **216**, 475–485.
Drew, H. R. & Dickerson, R. E. (1981). *J. Mol. Biol.* **151**, 535–556.
Egli, M. & Gessner, R. V. (1995). *Proc. Natl Acad. Sci. USA*, **92**, 180–184.
Egli, M., Williams, L. D., Gao, Q. & Rich, A. (1991). *Biochemistry*, **30**, 11388–11402.
Feigon, J., Wang, A. H., van der Marel, G. A., Van Boom, J. H. & Rich, A. (1984). *Nucleic Acids Res.* **12**, 1243–1263.
Forsyth, V. T., Mahendrasingam, A., Pigram, W. J., Greenall, R. J., Bellamy, K. A., Fuller, W. & Mason, S. A. (1989). *Int. J. Biol. Macromol.* **11**, 236–240.
Fujii, S., Wang, A. H.-J., van der Marel, G., van Boom, J. H. & Rich, A. (1982). *Nucleic Acids Res.* **10**, 7879–7892.
Fuller, W., Forsyth, T. & Mahendrasingam, A. (2004). *Philos. Trans. R. Soc. London B*, **359**, 1237–1248.
Fuller, W., Forsyth, V. T., Mahendrasingam, A., Pigram, W. J., Greenall, R. J., Langan, P., Bellamy, K. A., Al-Hayalee, Y. & Mason, S. A. (1989). *Physica B*, **156/157**, 468–470.
Fuciarelli, A. F., Wegher, B. J., Blakely, W. F. & Dizdaroglu, M. (1990). *Int. J. Radiat. Biol.* **58**, 397–415.
Gessner, R. V., Frederick, C. A., Quigley, G. J., Rich, A. & Wang, A. H. (1989). *J. Biol. Chem.* **264**, 7921–7935.
Gessner, R. V., Quigley, G. J. & Egli, M. (1994). *J. Mol. Biol.* **236**, 1154–1168.
Langan, P., Forsyth, V. T., Mahendrasingam, A., Pigram, W. J., Mason, S. A. & Fuller, W. (1992). *J. Biomol. Struct. Dyn.* **10**, 489–503.
Leslie, A. G., Arnott, S., Chandrasekaran, R. & Ratliff, R. L. (1980). *J. Mol. Biol.* **143**, 49–72.
Lipps, H. J., Nordheim A., Lafer, E. M., Ammermann, D., Stollar, B. D. & Rich, A. (1983). *Cell*, **32**, 435–441.
Liu, L. F. & Wang, J. C. (1987). *Proc. Natl Acad. Sci. USA*, **20**, 7024–2027.
Luzzati, V. (1952). *Acta Cryst.* **5**, 802–810.
McRee, D. E. Jr (1999). *J. Struct. Biol.* **125**, 156–165.
Maeda, M., Chatake, T., Tanaka, I., Ostermann, A. & Niimura, N. (2004). *J. Synchrotron Rad.* **11**, 41–44.
Malinina, L., Tereshko, V. & Ivanova, Z. (1991). *J. Cryst. Growth*, **110**, 252–257.
Matsuo, H., Oe, M., Sakiyama, F. & Narita, K. (1972). *J. Biochem.* **72**, 1057–1060.
Mizuno, N., Voordouw, G., Miki, K., Sarai, A. & Higuchi, Y. (2003). *Structure*, **11**, 1133–1140.
Ostermann, A., Tanaka, I., Engler, N., Niimura, N. & Parak, F. E. (2002). *Biophys. Chem.* **95**, 183–193.
Otwinowski, Z. & Minor, W. (1997). *Methods Enzymol.* **276**, 307–326.
Park, E. M., Shigenaga, M. K., Degan, P., Korn, T. S., Kitzler, J. W., Wehr, C. M., Kolachana, P. & Ames, B. N. (1992). *Proc. Natl Acad. Sci. USA*, **89**, 3375–3379.
Rich, A. & Zhang, S. (2003). *Nature Rev. Genet.* **4**, 566–572.
Schroth, G. P., Chou, P. J. & Ho, P. S. (1992). *J. Biol. Chem.* **267**, 11846–11855.
Schwartz, T., Behlke, J., Lowenhaupt, K., Heinemann, U. & Rich, A. (2001). *Nature Struct. Biol.* **8**, 761–765.
Schwartz, T., Rould, M. A., Lowenhaupt, K., Herbert, A. & Rich, A. (1999). *Science*, **284**, 1841–1845.
Shotton, M. W., Pope, L. H., Forsyth, T., Langan, P., Denny, R. C., Giesen, U., Dauvergne, M.-T. & Fuller, W. (1997). *Biophys. Chem.* **69**, 85–96.
Shotton, M. W., Pope, L. H., Forsyth, V. T., Langan, P., Grimm, H., Rupprecht, A., Denny, R. C. & Fuller, W. (1998). *Physica B*, **241–243**, 1166–1168.
Tanaka, I., Kurihara, K., Chatake, T. & Niimura, N. (2002). *J. Appl. Cryst.* **35**, 34–40.
Teeter, M. M. & Kossiakoff, A. A. (1984). *Basic Life Sci.* **27**, 335–348.
Tereshko, V., Wilds, C. J., Minasov, G., Prakash, T. P., Maier, M. A., Howard, A., Wawrzak, Z., Manoharan, M. & Egli, M. (2001). *Nucleic Acids Res.* **29**, 1208–1215.
Thamann, T. J., Lord, R. C., Wang, A. H. & Rich, A. (1981). *Nucleic Acids Res.* **9**, 5443–5457.
Tsunoda, M., Karino, N., Ueno, Y., Matsuda, A. & Takenaka, A. (2001). *Acta Cryst.* D**57**, 345–348.
Wang, A. H., Quigley, G. J., Kolpak, F. J., Crawford, J. L., van Boom, J. H., van der Marel, G. & Rich, A. (1979). *Nature (London)*, **282**, 680–686.
Wood, M. L., Dizdaroglu, M., Gajewski, E. & Essigmann, J. M. (1990). *Biochemistry*, **29**, 7024–7032.